

Development of CO₂ Chemical Absorbents Aided by Quantum Chemical Calculations in the COURSE50 Project

Yoichi MATSUZAKI*

Abstract

In the COURSE50 project, we have developed highly efficient CO₂ absorbents capable of decreasing the energy consumption associated with CO₂ separation. We also developed novel catalysts that effectively promote CO₂ absorption in practical absorbents. These studies have been aided by quantum chemical calculations.

1. Introduction

In its COURSE50 project (CO₂ Ultimate Reduction System for Cool Earth 50), the Japanese steel industry has been conducting research and development to reduce its CO₂ emissions by 30%: 10% by increasing the use of hydrogen reduction and 20% by capturing CO₂ in the blast furnace gas. As one of the latter initiatives, Nippon Steel Corporation and the Research Institute of Innovative Technology for the Earth (RITE) have been jointly developing the technology for capturing CO₂ by chemical absorption. The chemical absorption process that uses chemical reactions can absorb a large amount of CO₂ and can be easily scaled up. It can be applied to large CO₂ emission sources like blast furnaces and thermal power plants. The above-mentioned 20% reduction of CO₂ emissions translates to 3 Mt-CO₂/y at an 8 Mt/y steelworks. This volume of CO₂ can be processed with three 3 000 t-CO₂/d chemical absorption plants. Exhaust gases from blast furnaces and thermal power plants are at normal pressure. Their CO₂ concentrations are low at 22% and 10%, respectively. The chemical absorption process is effective for exhaust gases with such low CO₂ concentrations.

In Step 1 of Phase I of the project (2008 to 2012), we optimized aqueous absorbents and developed four new absorbents (RN-1 to RN-4). Nippon Steel Engineering Co., Ltd. commercialized a chemical absorption system by utilizing the development results. Here we sequentially introduce basic experimental and computational studies on which the development results are based; development of high-performance absorbents by using a laboratory scale test plant; pilot testing for actual blast furnace gas. The project is distinctive in that the quantum chemical calculation is used in basic research. The quantum chemical calculation is applied to clarify the mechanism of CO₂ absorption reaction, designing new amine compounds, and to search for absorption promoting catalysts as described later. Today, the quantum chemical calculation and other computational chemis-

try methods are indispensable in the development of functional materials. The Nippon Steel Group has applied the computational chemistry methods to various problems.

In Step 2 of Phase I of the project (2013 to 2017), we studied a wide range of innovative technologies, such as utilization of non-aqueous solvents, utilization of phase separation phenomena, and utilization of CO₂ absorption promoting catalysts. In Step 1 of Phase II (2018 to 2022), we have been tackling the ultimate search for absorbent performance. Of these research and development efforts currently underway, the development of CO₂ absorption catalysts is introduced in this paper.

2. Main Subjects

2.1 Principle and issues of chemical absorption process

Figure 1 schematically illustrates the chemical absorption process. In the absorber, the absorbent (aqueous solution of amine compound) countercurrently contacts the exhaust gas. The CO₂ in the exhaust gas is selectively absorbed according to the chemical reactions described later. The CO₂ rich absorbent is transferred to the stripper. When the absorbent is heated to about 120°C, it releases CO₂ and is regenerated. The purity of the recovered CO₂ is usually 99.9% or more. The regenerated absorbent is returned back to the absorber. This cycle is continuously repeated.

The absorption reaction is exothermic and can absorb a large amount of CO₂ due to its driving force. A large amount of the thermal energy (hereinafter referred to as the regeneration energy) is consumed in the stripper. The cost of the regeneration energy accounts for a large part of the capture cost. The regeneration energy is broken down into the reaction heat Q_R (the CO₂ desorption reaction is endothermic and thermal energy must be supplied to account for the heat lost), the sensible heat Q_S of the absorbent, and the latent heat Q_V of the vapor at the top of the stripper. These amounts of heat

* Chief Researcher, Dr. Eng., Mathematical Science & Technology Research Lab., Advanced Technology Research Laboratories
20-1 Shintomi, Futtsu City, Chiba Pref. 293-8511

greatly depend on the properties of the absorbent. The improvement of the absorbent is a key to reducing the regeneration energy. As shown in Fig. 2, the ratio of the reaction heat is generally high. It is most effective for reducing the reaction heat. As the CO₂ cyclic capacity per unit volume of the absorbent increases, the amount of the absorbent can be decreased. This in turn helps to reduce Q_S. If the regeneration temperature of the absorbent can be lowered, Q_V can be reduced. At the same time, more of the untapped waste heat at the steelworks can be utilized. Since reducing Q_R is generally associated with reduced reactivity, the CO₂ absorption rate is consequently reduced. As the absorption rate decreases, the actual CO₂ cyclic capacity decreases. The amount of the absorbent must be increased as a result. Therefore, Q_S increases and the absorber must be enlarged. How to eliminate this essentially trade-off relationship is a key point of the absorbent development.

Figure 2 shows the change in the absorbent performance. In Step 1 of Phase I, the final CO₂ separation and recovery energy target was set at 2.0 GJ/t-CO₂ or one half of the energy required for the MEA absorbent, through the improvement of the absorbent and the process. The development of new high-performance aqueous absorbents was conducted. (Note that the process improvement shown in Fig. 2 is not included.) In Step 2 of Phase I, the aforementioned innovative technologies were extensively studied to achieve a further reduction in the separation and recovery energy. In Step 1 of Phase II, we have searched for the ultimate absorbent performance, mainly by using promising seed technologies obtained then. We have been conducting research and development to achieve 1.6 GJ/t-CO₂, a

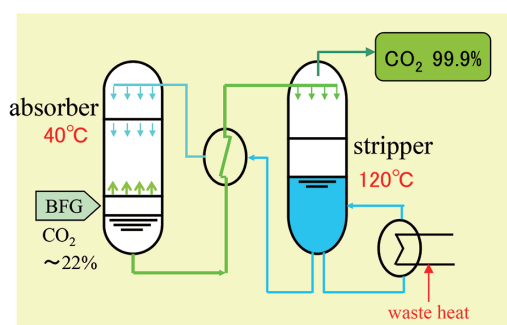
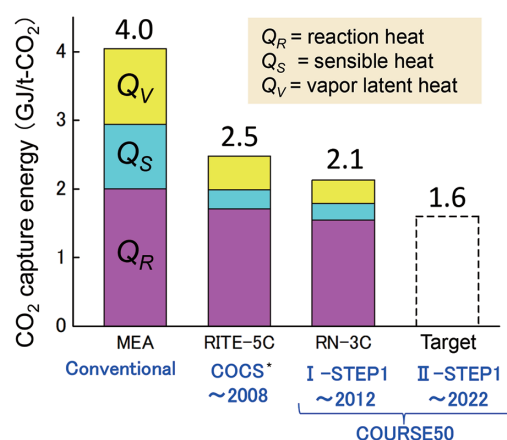


Fig. 1 Outline of chemical absorption process



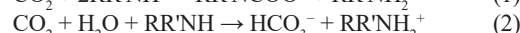
*COCS (Cost Saving CO₂ Capture System by Utilizing Low-grade Waste Heat)

Fig. 2 Reducing CO₂ capture energy by developing new absorbents

value close to the limit for practical absorbents.

2.2 Relationship between amine molecular structure and CO₂ absorption and desorption characteristics

CO₂ absorbents are generally aqueous solutions of amine compounds. When primary or secondary amines are used, the following reactions (1) and (2) coexist. CO₂ is absorbed as carbamate (RR'NCOO⁻) and bicarbonate (HCO₃⁻). When tertiary amine is used as the absorbent, reaction (2) alone occurs.



The molar ratio of CO₂ to amine is 1:2 for reaction (1) and 1:1 for reaction (2). The absorption efficiency is higher for the bicarbonate form.

We conducted CO₂ absorption and desorption experiments by using aqueous amine solutions shown in Fig. 3.¹⁾ The experimental results are also shown in Fig. 3. When we focus on monoethanolamine (MEA) (primary), diethanolamine (DEA) (secondary), and methyldiethanolamine (MDEA) (tertiary), typical examples of the respective classes of amines, we can confirm that the reaction heat and the absorption rate are actually in a trade-off relationship. The amines in the red-bordered box in Fig. 3 each have a bulky substituent near the nitrogen atom that is the reaction center. This type of amine is called a sterically hindered amine. The CO₂ cyclic capacity increases with the use of the sterically hindered amine AMP with respect to MEA. This is also true when IPAE is used with respect to DEA. Figure 4 shows the ratio of carbamate to bicarbonate determined by ¹³C-NMR spectroscopy. The bicarbonate form was found to be predominant in the sterically hindered amines. Since the bicarbonate form has a high absorption efficiency as noted above, the CO₂ cyclic capacity is considered to increase with the sterically hin-

Tertiary amine	Secondary amine	Primary amine
<chem>HOCH2CH2N(CH2CH2OH)2</chem> MDEA	<chem>HOCH2CH2N(CH2CH2OH)2</chem> DEA	<chem>NCCO</chem> MEA
	<chem>CC(C)(O)NCCO</chem> IPAE	<chem>CC(C)(O)NCCO</chem> AMP

Sterically hindered amine

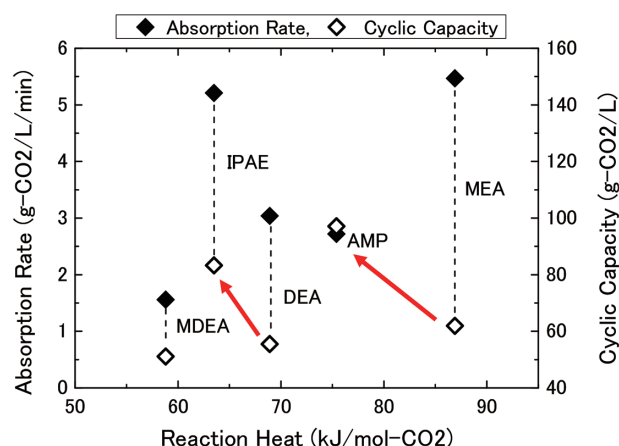


Fig. 3 (Upper) Molecular structure of amine compounds (Lower) CO₂ absorption characteristics of aqueous amine solutions

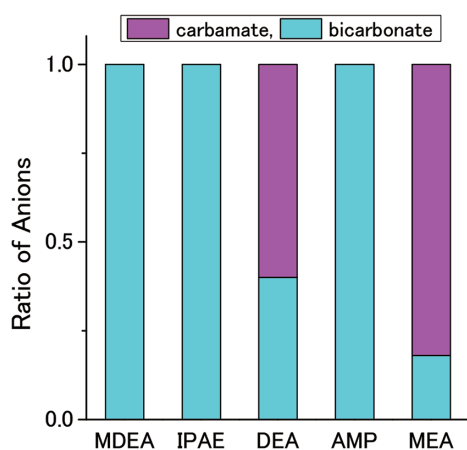


Fig. 4 ¹³C-NMR speciation of reaction products

dered amines.

2.3 Quantum chemical calculation of reaction mechanism concerning sterically hindered amines

A conventional reason for the difficulty of carbamate forming in the sterically hindered amines is as follows: The carbamate is destabilized by the steric hindrance. The hydrolysis reaction of Equation (3) (= (2) – (1)) thus easily proceeds and carbamate changes to bicarbonate.²⁾



According to the x-ray structure analysis of the AMP carbamate, however, no significant elongation of the N-C bond is observed.³⁾ It is thus difficult to consider that a large steric repulsion acts from the methyl group. Furthermore, our quantum chemical calculation showed that the activation energy of Equation (3) is very large for both MEA and AMP and that the reaction proceeds negligibly.^{4,5)} There are some studies that point to factors other than the steric hindrance. According to analysis by semiempirical molecular orbital calculation, it is pointed out that the electron donation of the methyl group makes the N atom a “softer” base and lowers its affinity with CO₂, a “hard” acid.⁶⁾ From a recent first principles molecular dynamics simulation, another mechanism is proposed.⁷⁾ According to the mechanism, the solvation around the N atom is stronger for AMP than for MEA. It inhibits access to CO₂. At the same time, the deprotonation of H₂O promotes the formation of the OH⁻ ions. Accordingly, the formation of the bicarbonate is kinetically more advantageous than that of the carbamate. The sterically hindered

amines are extremely important absorbent components thanks to their excellent properties. As described above, however, their performance development mechanism is not yet properly understood.

Based on recent experimental and computational results, we decided to study the performance development mechanism of the sterically hindered amines. Ciftja et al.⁸⁾ confirmed by NMR spectroscopy that the carbamate of AMP is actually formed until the mol loading reaches 0.5 and then continues to decrease. Finally, the bicarbonate alone exists. This suggests that carbamate is transformed to bicarbonate. However, the reaction of Equation (3) does not directly occur in this transformation. It is considered instead that the reverse reaction of Equation (1) forms free CO₂ and then promotes reaction (2) (Fig. 5).⁴⁾ Reaction (1) is actually a two-step reaction via a zwitterionic intermediate. The two steps are written as (-1a) and (-1b) in Fig. 5 (the minus signs indicate reverse reactions). We analyzed the chemical equilibrium of elementary reactions on the reaction pathway of Fig. 5 and investigated how the substituent near the N atom shifts the overall chemical equilibrium to the bicarbonate.⁹⁾

The Gaussian 09 program¹⁰⁾ was used for the quantum chemical calculations. The optimization of the molecular structure was conducted by MP2/6-311++G(d,p), the single-point energy calculation at the optimized structure was performed by CCSD(T)/6-311++G(2df,2p), and the solvent effect was considered by the SMD continuum dielectric model.

First, the free energy change ΔG of reaction (3) at 30°C was calculated and compared with the experimental values to verify the calculation accuracy. The calculated values of ΔG in kcal/mol (4.32 for MEA and 1.28 for AMP) agree well with the experimental values (4.56 for MEA and <1.45 for AMP). This method is considered to be effective for the analysis described below.

Next, ΔG was calculated for the elementary reactions on the actual reaction pathway. Since the ideal gas model was used to calculate G , the effect of the translational entropy is overestimated in cases where the number of molecules changes before and after the reaction. Therefore, we focus on $\Delta\Delta G = \Delta G(\text{AMP}) - \Delta G(\text{MEA})$ below. It is sufficient to discuss the difference between MEA and AMP. When we looked at $\Delta\Delta G$ of the elementary reactions, we found that the shift of the equilibrium of (1b) to the zwitterion form is the largest factor for the shift of the carbamate-bicarbonate equilibrium for AMP rather than for MEA. The equilibrium of elementary reaction (1b) depends on the basicity difference between the free amine and the carbamate. This means that the increase of basicity by the two methyl groups is more pronounced in the carbamate than in the free amine. This effect of the methyl groups is considered to be due to

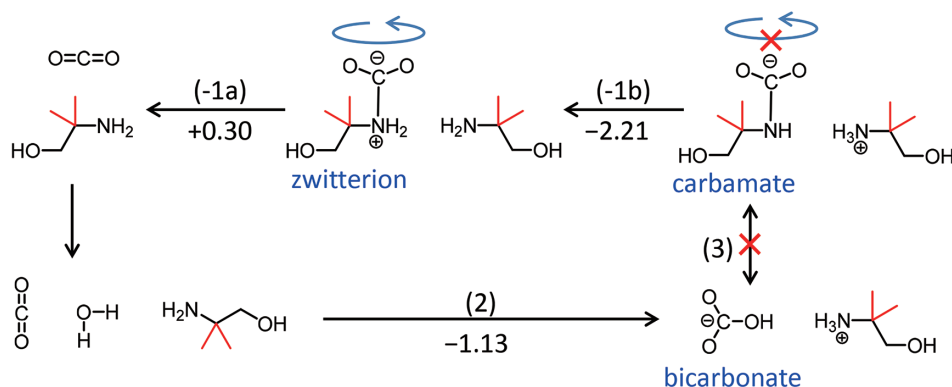


Fig. 5 Reaction pathway from carbamate to bicarbonate

the electronic effect rather than to the steric hindrance. This is because the optimized N-C bond length of the carbamate is almost the same for MEA (1.409Å) and AMP (1.410Å), but also because the behavior of the electronic state of the N atom agrees with the aforementioned basicity tendency. That is, according to the quantum chemical calculation, the increase in the negative charge on the N atom due to the methyl group is larger in the carbamate (0.149) than in the free amine (0.123). The increase in the lone-pair orbital energy is also greater than in the carbamate (0.112 eV) than in the free amine (0.108 eV). These correspond to the larger increase in the basicity with the carbamate. As for the other elementary reactions, the equilibrium of elementary reaction (1a) shifts slightly to the zwitterion side for AMP as compared to MEA. The equilibrium of elementary reaction (2) shifts to the bicarbonate side for AMP, which contributes to the equilibrium shift from the carbamate to the bicarbonate, although not as much as elementary reaction (1b) does.

The above-mentioned analysis of the effect of methyl groups is based on the most stable structure. Concerning the steric effect, it is also necessary to consider dynamics such as conformational change. In this study, we focused on the rotation of the OCO moieties of the carbamate and the zwitterion. This rotation is expected to have a large effect (Fig. 5). **Figure 6** shows the calculated energy change associated with the rotation of the OCO moiety. Such a motion is suppressed in the carbamate, but the energy barrier of rotation is found to be about 3 kcal/mol for the zwitterion. Therefore, we examined the conformation of the zwitterion. We found that in the structure shown on the right side of Fig. 6, the H atom of the methyl group and the O atom of the OCO moiety approach up to 1.435 Å. The distance between the H atom and the O atom is much shorter than the sum of the van der Waals radii of the O and H atoms (2.6 Å). This structure corresponds to 180° along the horizontal axis of

the left graph of Fig. 6. The energy increase from the most stable conformation, including the conformational changes of other moieties, is about 10 kcal/mol. There is a good chance that the zwitterion may instantaneously undertake such a conformation at an operating temperature of about 40°C. At that time, CO₂ may be expelled by the steric repulsion from the methyl group. Ma et al.¹¹⁾ reported that the CO₂ desorption reaction from the MEA carbamate passes through the zwitterion according to the first principles molecular dynamics calculation. It is interesting to see if the above dynamic effect of methyl groups is observed when a similar simulation is performed with AMP.

In addition to the above-mentioned substituent effect, the alcohol chain length of alkanolamine has a great influence on the formation ratio of carbamate and bicarbonate. We clarified by ¹³C-NMR spectroscopy that the formation ratio of carbamate decreases with the increase in the alcohol side chain length and conducted analysis focusing on the intramolecular hydrogen bond of carbamate by using the quantum chemical calculation.¹²⁾ We also reported the experimental study of the CO₂ absorption and desorption characteristics of linear amines and cyclic amines.¹³⁾

2.4 Development of new high-performance absorbents

The basic experiments and quantum chemical calculations described in the previous section showed that the sterically hindered amines are effective in improving the properties of the absorbents. We further optimized the molecular structures of sterically hindered amines.¹⁴⁾ We adjusted the performance of absorbents with a blend of two or more amines and optimized absorbent compositions. In this way, we developed a total of four new RN series absorbents. The properties of the new absorbents are compared with those of conventional absorbents MEA and RITE-5C in **Table 1**. The RITE-5C absorbent has the highest performance of the absorbents devel-

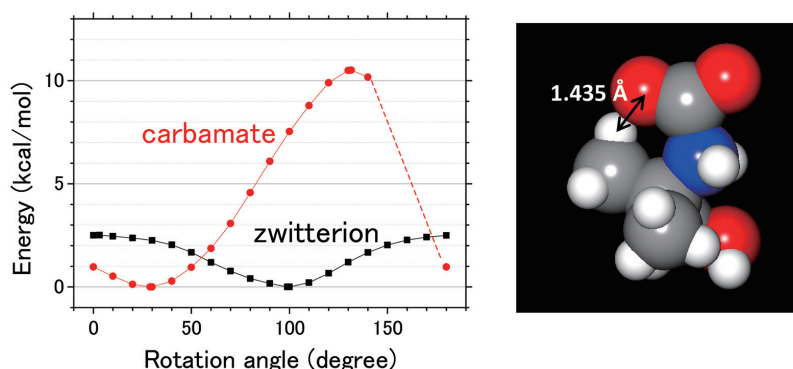


Fig. 6 (Left) Calculated potential energy with respect to rotation of OCO moiety (Right) Calculated structure of AMP zwitterion with hindered conformation

Table 1 Lab-scale performances of RN-series absorbents

Absorbents	Absorption rate (g/L/min)	Cyclic capacity* (g/L)	Reaction heat (kJ/mol-CO ₂)	CO ₂ capture energy (GJ/t-CO ₂)	
				CAT-LAB	Math. model
RN-1B	4.2	152	71	2.81	2.3
RN-2F	4.6	155	71	2.76	2.3
RN-3C	4.5	149	68	2.52	2.1
RN-4B'	4.3	154	68	2.36	2.0
RITE-5C	5.0	132	75	3.03	2.5
MEA 30wt%	5.5	62	87		4.0

* Difference in CO₂ loading between 40°C and 120°C under equilibrium condition.

oped by the RITE before the COURSE50 project.¹⁵⁾ The RN series absorbents have a larger CO₂ cyclic capacity and a lower reaction heat than those of the RITE-5C absorbent. When we looked at the temperature dependence of the CO₂ loading by the vapor-liquid equilibrium measurement in Fig. 7, we found that the RN series absorbents can be regenerated at a lower temperature than the RITE-5C absorbent.

We evaluated the performance of the RN series absorbents by using the laboratory-scale continuous test plant CAT-LAB of Fig. 8 with a 5 kg-CO₂/d capacity. The heat was supplied to the stripper by using an electric heater. The energy input to a reboiler was measured with a wattmeter and divided by the CO₂ loading to calculate the regeneration energy. We built a heat and mass balance calculation model by using the vapor-liquid equilibrium characteristics and the reaction heat of the CO₂ absorbents measured during a laboratory physical property evaluation test. Using the model, we evaluated the potential of the new absorbents to reduce the CO₂ separation and recovery energy. In this study, the stripper is analyzed by the stage

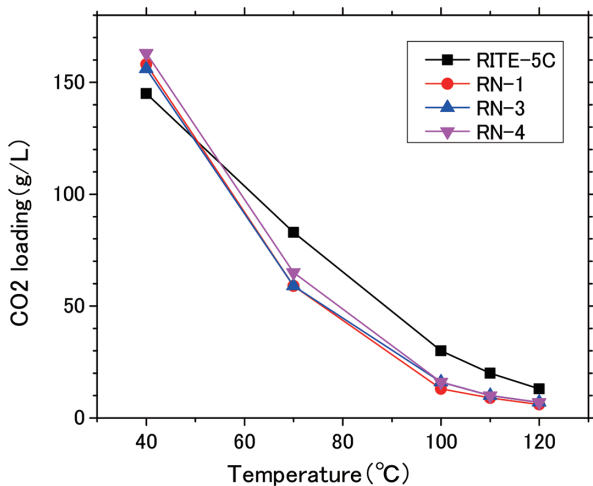


Fig. 7 Temperature dependence of CO₂ loading

calculation (heat and mass balance calculation) based on vapor-liquid equilibrium data. This evaluation method is called an “equilibrium model”.

Table 1 shows the evaluation results of CO₂ regeneration energy by the CAT-LAB and the equilibrium model. The CO₂ regeneration energy was reduced further as the new absorbents were changed from RN-1 to RN-2, -3, and -4 in the development stages. The CAT-LAB data shown here were obtained under such operating conditions that the stripper reboiler temperature (absorbent regeneration temperature) was 100°C or more. From the properties of the above-mentioned RN absorbents, it was found that the separation and recovery energy can be reduced further when the regeneration temperature is set to less than 100°C. These test results will be reported together with the performance of the latest absorbents on another occasion. According to the results calculated with the equilibrium model and shown in Table 1, the RN-4 absorbent has the potential to achieve a regeneration energy of 2.0 GJ/t-CO₂.

2.5 Bench and pilot tests

Based on the results of the laboratory scale test described above, in Step 1 of Phase I, Nippon Steel Engineering conducted bench scale (CAT1; 1 t-CO₂/d capacity) and pilot scale (CAT30; 30 t-CO₂/d capacity) tests by using the exhaust gas of a blast furnace.¹⁶⁾ The absorbents used in the tests were the RN-1 and RN-3 absorbents. The CAT30 test confirmed that the regeneration energy of the RN-3C absorbent can be reduced to 2.34 GJ/t-CO₂ and that the regeneration temperature of the RN-3C absorbent can be lowered from 120°C to 95°C. The 2000-h CAT30 test found no increase in the regeneration energy. The RN-1 and RN-3 absorbents were demonstrated to have extremely high durability. It was also confirmed that the RN-1 and RN-3 absorbents have no operation problems and have little equipment corrosion as compared with conventional MEA-based absorbents. After the above-mentioned tests, the RN absorbents were adopted by Nippon Steel Engineering’s energy saving CO₂ absorption process (ESCAP). Two commercial ESCAP plants are currently in operation.

2.6 Development of next-generation absorbents

The above-mentioned development found the limit to the reduction of the regeneration energy with conventional absorbents. We

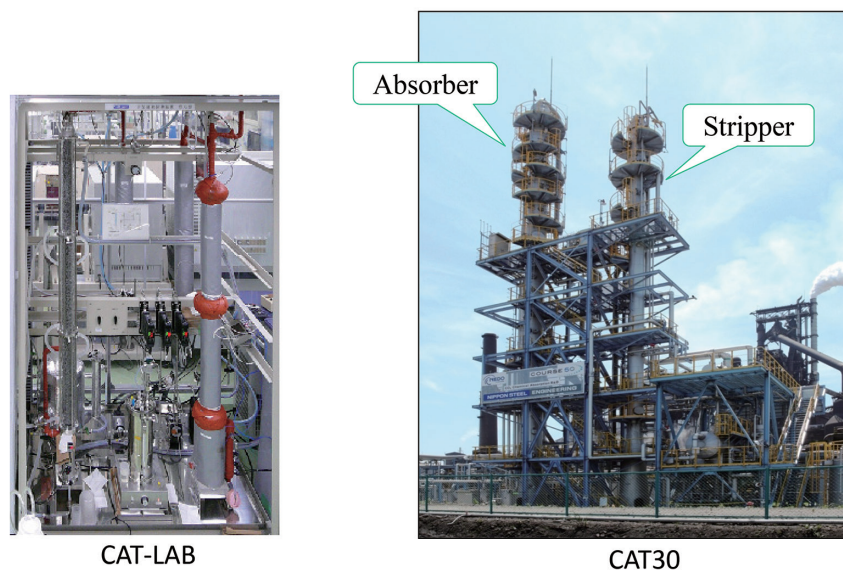


Fig. 8 Test equipment in chemical absorption process

are therefore aiming to further reduce the regeneration energy by examining various innovative technologies and concentrating on promising technologies thus found. Particularly to reduce the reaction heat that accounts for most of the regeneration energy, we have studied how to alleviate the solvation effect by using nonaqueous solvents and how to reduce the reaction heat to the utmost limit.¹⁷⁾ On the other hand, however, the reduction of the reaction heat inevitably leads to a decrease in the reaction rate (absorption rate). Catalysts have hence assumed ever greater importance to counter this situation. Our search for catalysts by utilizing quantum chemical calculation is described below.

2.7 Search for absorption-promoting catalysts¹⁸⁾

Carbonic anhydrases (CA) accelerate the CO₂ absorption reaction. Studies have been conducted on CO₂ capture processes using CA. However, enzymes have problems with stability at high temperatures. We focused on metal complexes that mimic the active center of CA. Many such metal complexes have already been reported. As a typical example, the metal complex ZC (Fig. 9) is reported to have an excellent catalytic effect in a dilute solution.^{19, 20)} So, we evaluated the effect of ZC addition to a 30 wt% aqueous solution of isopropylaminoethanol. Contrary to our expectation, we saw no improvement at all in the absorption rate.

The mechanism of Fig. 10 is proposed for the catalytic reaction of CA and ZC. In the case of ZC, the rate-determining step is considered to be (4) (the formed HCO₃⁻ is desorbed from the catalyst and a free catalyst is regenerated).²¹⁾ Considering this and the fact that the HCO₃⁻ is formed in a large amount in the absorbent of high-concentration amine, it is presumed that the catalytic effect of ZC did not appear due to so-called product inhibition.^{22, 23)}

For the catalytic effect to appear, therefore, it is necessary to use

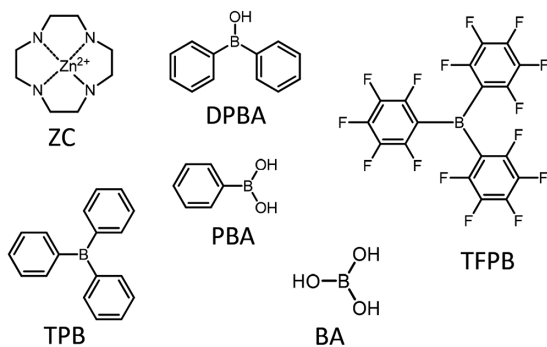


Fig. 9 Molecular structures of catalysts

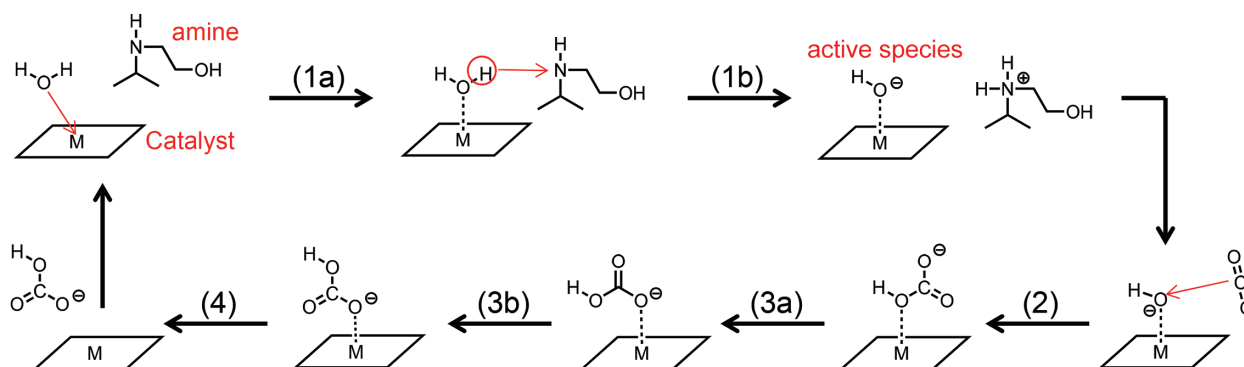


Fig. 10 Illustration of catalytic reaction cycle of catalysts

a catalyst with a stronger affinity for OH⁻ than for HCO₃⁻. When we focus on the fact that metal atoms in catalysts are Lewis acids and that oxygen atoms of the active species OH⁻ and the product HCO₃⁻ are Lewis bases, we can apply the hard and soft acids and bases (HSAB) principle for the acid-base interaction. That is, because OH⁻ is a harder base than HCO₃⁻, a hard Lewis acid should be effective if the affinity with OH⁻ is strengthened.

We performed the same test on TFPB as we did on ZC (Fig. 9). TFPB is a hard acid. We saw no improvement in the absorption rate as shown in Fig. 11. (The absorption rate is the slope of each absorption curve.) We therefore decided to clarify the conditions for the catalytic effect to appear and to obtain the guideline for searching catalysts by using quantum chemical calculations. The conditions under which the catalytic effect appears are: (1) active species are thermodynamically more stable than reaction products and (2) the active species and CO₂ have high reaction rates. Regarding condition (1), the effective binding energy of OH⁻ ions in the active species is defined as $G_b^{eff}(\text{OH}^-) \equiv -(\Delta G[1a] + \Delta G[1b])$ ($\Delta G[1a]$ and $\Delta G[1b]$ are the free energy changes of reactions (1a) and (1b) in Fig. 10, respectively). $G_b(\text{HCO}_3^-) - G_b^{eff}(\text{OH}^-)$ was used as an index. $G_b(\text{HCO}_3^-)$ is the binding energy between HCO₃⁻ and the catalyst. For condition (2), the activation free energy (ΔG^\ddagger) of reaction (2) in Fig. 10 was used as an index.

When we calculated both indexes for TFPB, we found that the resistance to inhibition of TFPB is certainly improved as compared with ZC, but that its reactivity with CO₂ is significantly reduced.

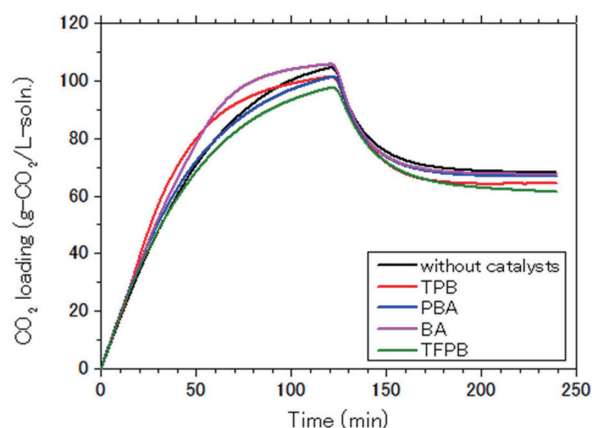


Fig. 11 CO₂ absorption-regeneration profiles for amine absorbents with and without catalysts

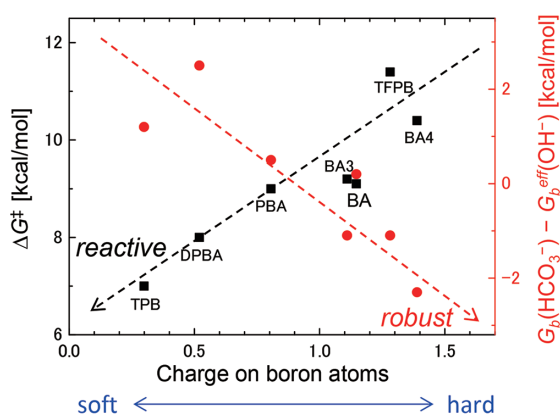


Fig. 12 Calculated key reaction characteristics plotted against hardness of boron centers

Actually, the ΔG^\ddagger of TFPB is almost the same as the ΔG^\ddagger of the CO_2 absorption reaction by amines. This suggests that the above requirements (1) and (2) are in a trade-off relationship; that is, the harder the acid, the better the resistance to inhibition, but the lower the reactivity with CO_2 . We then targeted boron compounds that are softer than TFPB and predicted by the quantum chemical calculation the catalyst performance index for TPB, DPBA, PBA, and BA (boric acid) in Fig. 9. As a result, the above-mentioned trade-off relationship is certainly established as shown in Fig. 12. We found that these boron compounds are expected to have better reactivity with CO_2 than TFPB. We conducted a verification experiment of the catalytic effect of commercially available TPB, PBA, and BA. As a result, we confirmed the effect of each improving the absorption rate as shown in Fig. 11. The absorption rate improvement was highest for TPB at 50% saturated absorption. On the other hand, BA is characterized by its greater effect in the latter half of the absorption stage than TPB. TPB is insoluble in water, but BA is water soluble. BA is thus considered to be more evenly dispersed in the solution. In general, absorbents increase in viscosity as they absorb CO_2 . We thus consider that water-soluble catalysts are advantageous in terms of the reaction probability with CO_2 .

3. Conclusions

We introduced here the development of CO_2 absorbents we have jointly undertaken with RITE in the COURSE50 project. We focused on the results of Step 1 of Phase I as well as the catalysts developed subsequently. Although there already are commercialized chemical absorption technologies, the absorbent regeneration cost must be reduced further for greater use of chemical absorption. Now, the COURSE50 project aims to pursue the ultimate performance of the absorbents and to reduce the regeneration energy close to the lowest possible limit by fiscal 2022.

In this paper, we also strongly recognized the need for the social implementation of the quantum chemistry calculation and described

in detail how to utilize it in the studies to prevent global warming. To build a sustainable society, we have little time left to solve environmental and energy problems. Chemistry plays a central role in solving these problems. As long as quantum chemistry is its theoretical foundation, the importance of the quantum chemical calculation cannot be overstated. Its contribution should increase even further in the future. We would like to play a part in that endeavor.

Acknowledgements

This work was financially supported by the COURSE50 project founded by the New Energy and Industrial Technology Development Organization, Japan.

References

- 1) Chowdhury, F.A., Goto, K., Yamada, H., Matsuzaki, Y., Yamamoto, S., Higashii, T., Onoda, M.: Energy Procedia. 114, 1716–1720 (2017)
- 2) Sartori, G., Savage, D.W.: Ind. Eng. Chem. Fundam. 22, 239–249 (1983)
- 3) Jo, E., Jhon, Y.H., Choi, S.B., Shim, J-G., Kim, J-H., Lee, J.H., Lee, I-Y., Jang, K-R., Kim, J.: Chem. Commun. 46, 9158–9160 (2010)
- 4) Yamada, H., Matsuzaki, Y., Higashii, T., Kazama, S.: J. Phys. Chem. A 115, 3079–3086 (2011)
- 5) Matsuzaki, Y., Yamada, H., Chowdhury, F.A., Higashii, T., Onoda, M.: J. Phys. Chem. A 117, 9274–9281 (2013)
- 6) Chakraborty, A. K., Bischoff, K. B., Astarita, G., Damewood, J.R.: J. Am. Chem. Soc. 110, 6947–6954 (1988)
- 7) Stowe, H.M., Vilčiauskas, L., Paek, E., Hwang, G.S.: Phys. Chem. Chem. Phys. 17, 29184–29192 (2015)
- 8) Ciftja, A.F., Hartono, A., Svendsen, H.F.: Chem. Eng. Sci. 107, 317–327 (2014)
- 9) Matsuzaki, Y., Yamada, H., Chowdhury, F.A., Yamamoto, S., Goto, K.: Ind. Eng. Chem. Res. 58, 3549–3554 (2019)
- 10) Frisch, M.J. et al.: Gaussian 09, Revision E.01; Gaussian, Inc., Wallingford, CT, 2009
- 11) Ma, C., Pietrucci, F., Andreoni, W.: J. Chem. Theory Comput. 11, 3189–3198 (2015)
- 12) Yamada, H., Matsuzaki, Y., Chowdhury, F.A., Higashii, T.: J. Mol. Model. 19, 4147–4153 (2013)
- 13) Chowdhury, F.A., Yamada, H., Higashii, T., Matsuzaki, Y., Kazama, S.: Energy Procedia. 37, 400–406 (2013)
- 14) Yamada, H., Matsuzaki, Y., Okabe, H., Shimizu, S., Fujioka, Y.: Energy Procedia. 4, 133–139 (2011)
- 15) Goto, K., Okabe, H., Shimizu, S., Onoda, M., Fujioka, Y.: Energy Procedia. 1, 1083–1089 (2009)
- 16) Hayashi, M., Mimura, T.: Energy Procedia. 37, 7134–7138 (2013)
- 17) Chowdhury, F.A., Goto, K., Yamada, H., Matsuzaki, Y.: Int. J. Greenhouse Gas Control. 99, 103081 (2020)
- 18) Matsuzaki, Y., Yamamoto, S., Yamada, H., Chowdhury, F.A., Goto, K.: Ind. Eng. Chem. Res. 59, 13016–13023 (2020)
- 19) Zhang, X., van Eldik, R., Koike, T., Kimura, E.: Inorg. Chem. 32, 5749–5755 (1993)
- 20) Zhang, X., van Eldik, R.: Inorg. Chem. 34, 5606–5614 (1995)
- 21) Koziol, L., Valdez, C.A., Baker, S.E., Lau, E.Y., Floyd, W.C., III, Wong, S.E., Satcher, J.H., Jr, Lightstone, F.C., Aines, R.D.: Inorg. Chem. 51, 6803–6812 (2012)
- 22) Nakata, K., Shimomura, N., Shiina, N., Izumi, M., Ichikawa, K., Shiro, M.: J. Inorg. Biochem. 89, 255–266 (2002)
- 23) O'Donnely, K., Oliver, T., Woscholski, R., Long, N.J., Barter, L.M.C.: ACS Catal. 9, 1353–1365 (2019)



Yoichi MATSUZAKI
Chief Researcher, Dr. Eng.
Mathematical Science & Technology Research Lab.
Advanced Technology Research Laboratories
20-1 Shintomi, Futsu City, Chiba Pref. 293-8511